

Radiation Thermometry and Emissivity Measurements Under Vacuum at the PTB

C. Monte · B. Gutschwager · S. P. Morozova · J. Hollandt

Published online: 18 June 2008
© Springer Science+Business Media, LLC 2008

Abstract A new experimental facility was realized at the PTB for reduced-background radiation thermometry under vacuum. This facility serves three purposes: (i) providing traceable calibration of space-based infrared remote-sensing experiments in terms of radiation temperature from $-173\text{ }^{\circ}\text{C}$ to $430\text{ }^{\circ}\text{C}$ and spectral radiance; (ii) meeting the demand of industry to perform radiation thermometric measurements under vacuum conditions; and (iii) performing spectral emissivity measurements in the range from $0\text{ }^{\circ}\text{C}$ to $430\text{ }^{\circ}\text{C}$ without atmospheric interferences. The general concept of the reduced background calibration facility is to connect a source chamber with a detector chamber via a liquid nitrogen-cooled beamline. Translation and alignment units in the source and detector chambers enable the facility to compare and calibrate different sources and detectors under vacuum. In addition to the source chamber, a liquid nitrogen-cooled reference blackbody and an indium fixed-point blackbody radiator are connected to the cooled beamline on the radiation side. The radiation from the various sources is measured with a vacuum infrared standard radiation thermometer (VIRST) and is also imaged on a vacuum Fourier-transform infrared spectrometer (FTIR) to allow for spectrally resolved measurements of blackbodies and emissivity samples. Determination of the directional spectral emissivity will be performed in the temperature range from $0\text{ }^{\circ}\text{C}$ to $430\text{ }^{\circ}\text{C}$ for angles from 0° to $\pm 70^{\circ}$ with respect to normal incidence in the wavelength range from $1\text{ }\mu\text{m}$ to $1,000\text{ }\mu\text{m}$.

References to commercial products are provided for identification purposes only and constitute neither endorsement nor representation that the item identified is the best available for the stated purpose.

C. Monte (✉) · B. Gutschwager · J. Hollandt
Physikalisch-Technische Bundesanstalt, Abbestraße 2-12, 10587 Berlin, Germany
e-mail: christian.monte@ptb.de

S. P. Morozova
All-Russian Research Institute for Optical and Physical Measurement, Moscow, Russia

Keywords Blackbody · Emissivity · Radiation thermometry · Radiometry · Remote sensing · Vacuum

1 Introduction

The concept and design of the reduced background calibration facility (RBCF) resulted from demands from three areas:

1.1 Remote Sensing

In [1], the American Meteorological Society states the desired long-term stabilities and accuracies for climate variable datasets. The resulting accuracies and stabilities for the measurement of these variables by remote-sensing observations from space are equal to or sometimes smaller than these values. For spectrally resolved thermal radiance and for sea-surface temperature datasets, they require an uncertainty of 0.1 K and a stability of 0.04 K per decade, corresponding to 0.01 K measurement stability in the IR spectral band. Atmospheric variables such as tropospheric and stratospheric temperatures should be measured with an uncertainty of 0.5 K and a stability of 0.04 K. These values can only be reached by using either very stable detectors or onboard calibration sources, which in any case have to be calibrated to be traceable to the SI units of spectral responsivity, spectral radiance, spectral irradiance, or to the International Temperature Scale (ITS-90), by pre-flight and in-flight procedures. To minimize the measurement uncertainty in space, the pre-flight calibration has to be performed under similar conditions as found in space. With the vacuum reduced-background calibration facility, PTB is able to provide traceable calibration of space-based infrared remote-sensing experiments in terms of spectral radiance and radiation temperature from -170°C to 430°C .

1.2 Process Control

Commercial radiation thermometers cover the temperature range from -100°C to $3,000^{\circ}\text{C}$. Accurate calibrations at temperatures below the freezing point of water are difficult to perform in air due to the problem of moisture and ice build-up on the blackbody walls, even with purged radiators. For specific process control applications, especially in the semiconductor and glass industries, radiation thermometry is performed under vacuum conditions. Consequently, the RBCF will complement the PTB low-temperature calibration facility based on heat-pipe radiators that provide blackbody radiation in the temperature range from -60°C to 962°C under atmosphere [2].

1.3 Emissivity

Non-contact thermal monitoring (for example, in the areas of process and quality control, surveillance, security, food conservation, and heat insulation) requires accurate knowledge of the emissivity of the observed surface within the application's

temperature range. We will address this need by extending the temperature range of our conventional spectral emissivity measurements in air [3] down to 0°C with the RBCF. Several major difficulties have to be addressed for emissivity measurements at low temperatures to achieve sufficient uncertainty. One difficulty is the thermal radiation from the surroundings of the sample and from the Fourier-transform infrared spectrometer (FTIR). The problem of thermal radiation from the surroundings is addressed directly by the construction of the RBCF. All critical parts in the optical path are liquid nitrogen cooled. The remaining thermal radiation (for example, from the beam splitter of the FTIR) can be reduced by a measurement scheme that incorporates two blackbodies of different temperatures as reference sources (see Sect. 3.5). Another difficulty is the accurate determination of the surface temperature. In our case, this is done by balancing the heat flux through the sample with the heat loss from the sample surface [3].¹ Here, the major uncertainty results from the part of the model describing the convective heat loss from the sample surface when using the model with our conventional emissivity facility in air. By working under vacuum conditions with the RBCF, this problem is elegantly avoided and a precise determination of surface temperatures will be possible. Finally, changing atmospheric absorptions due to varying partial pressures of H₂O and CO₂, which commonly appear even in purged systems, cause additional and significant uncertainties in specific spectral ranges of the emissivity spectrum. An example of these disturbances with our conventional facility is shown in Fig. 1. This point will, of course, be avoided in a vacuum system.

2 Instrumentation

2.1 General Layout

The general concept of the RBCF is to connect several sources and detectors via a liquid nitrogen-cooled beamline (Figs. 2 and 3). The experimental setup incorporates parts of the VNIIOFI medium-background facility [4]. The liquid nitrogen-cooled beamline features a liquid nitrogen-cooled reference blackbody and an indium fixed-point blackbody radiator that are connected via an opto-mechanical unit to the beamline [4]. The radiation from these two blackbodies can be imaged via a reflective chopper wheel or a gold mirror on a translation stage, respectively, in the direction of the optical axis of the beamline. The beamline connects the newly designed source and detector chambers directly on its optical axis without needing a mirror. Linear translation units in the source and detector chambers enable the facility to compare and calibrate different sources and detectors under vacuum. By using vertical and angular translation stages

¹ Briefly: The thermal conductivity of the sample and of a possible coating are known. Using two temperature sensors in the heating plate and in the sample, the thickness of the air gap between the heating plate and the sample as well as the heat flow through the sample can be calculated. The heat loss from the sample surface is the sum of the radiative and convective heat losses. Because the surface temperature and emissivity of the surroundings are known, the radiative heat loss can be calculated from an assumed hemispherical emissivity and an assumed surface temperature of the sample. Also, the convective loss from the surface can be calculated for the assumed surface temperature. By balancing the overall heat loss with the heat flux through the sample, the surface temperature can be iteratively determined. In a second “outer” iteration, the assumed hemispherical emissivity is refined from the directional emissivities.

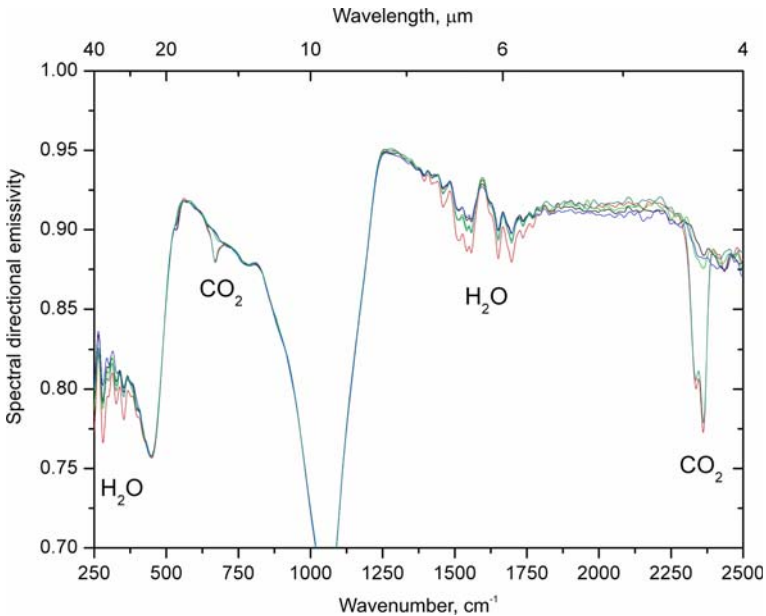


Fig. 1 Atmospheric interferences in a sequence of measurements of the directional spectral emissivity of a sample of BK7 glass in air observed at 5° to the surface normal. The delay between consecutive measurements was 5 min. The spectra were recorded with a purged spectrometer and equal path length in air to sample and reference blackbody, respectively. Due to the ratio measurement, in principle, remaining atmospheric interferences should cancel. However, this is only partly the case, as is clearly visible by the variation of the CO_2 and H_2O bands. The CO_2 distortion nearly disappears after 15 min whereas the H_2O distortion remains visible

in the detector chamber, it is possible to scan extended sources and detectors and measure their homogeneity.

In addition to the indium fixed-point blackbody, the standard reference sources of the RBCF are two dedicated vacuum variable-temperature blackbodies, the vacuum low-temperature blackbody (VLTBB, Fig. 4) and the vacuum medium-temperature blackbody (VMTBB, Fig. 5). Details to all blackbody radiators of the RBCF are given in Table 1. The VMTBB is still under construction while the VLTBB is in operation and described in detail in [5]. By using calibrated platinum resistance thermometers placed at the bottom and along the cavity walls of the VLTBB and VMTBB, their radiation temperatures are traceable to ITS-90. With the vacuum infrared standard radiation thermometer (VIRST) [6], the radiation temperature of the VLTBB has been directly compared to the low-temperature heat-pipe blackbodies of PTB that are the national primary standards of radiation temperature from -50°C to 962°C . Details are given in Sect. 3. The third position in the source chamber is occupied either by a source under test or by a specific sample holder for spectral emissivity measurements.

By using an off-axis ellipsoidal mirror that can be moved to the detector position on the optical axes of the RBCF, the radiation from the various sources can also be imaged on a vacuum FTIR to allow for spectrally resolved measurements of blackbodies and

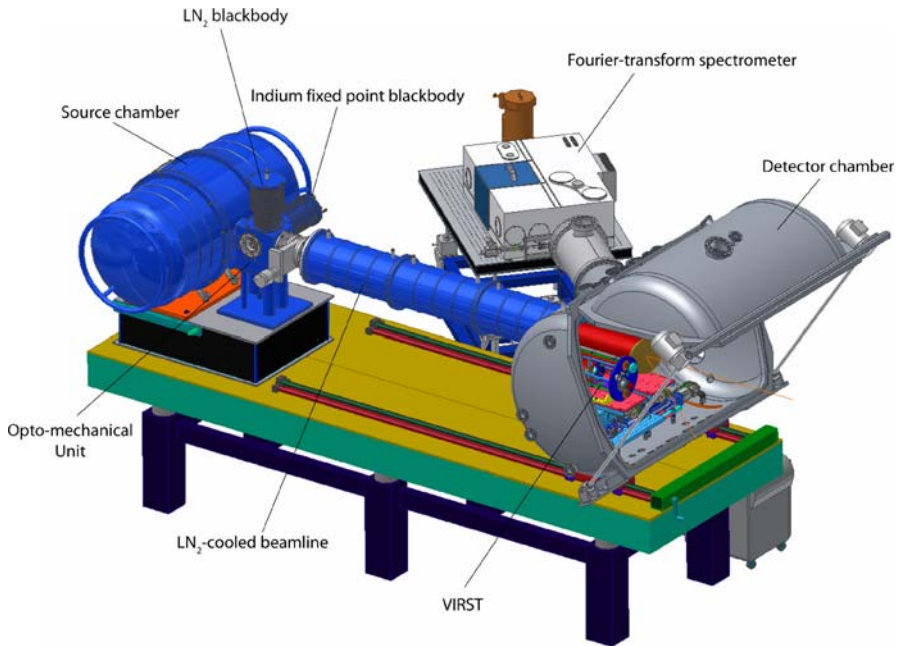


Fig. 2 Overview of the construction of the reduced-background calibration facility (RBCF). The source chamber is connected via the LN₂-cooled opto-mechanical unit and the beamline to the detector chamber. The LN₂-cooled blackbody and the indium fixed-point radiator are mounted on the opto-mechanical unit. They are imaged with a highly reflective chopper wheel, or a gold mirror mounted on a vertical translation stage, toward the detector chamber. In the opened detector chamber, VIRST and the off-axis ellipsoidal mirror are shown on their translation stages. In the background, the vacuum FTIR with the bolometer is shown

emissivity samples. In Fig. 3, the facility is shown partly transparent to illustrate the beam path for directional spectral emissivity measurements.

2.2 Components

2.2.1 Vacuum Variable Low-Temperature Blackbody (VLTBB)

The VLTBB is a reference blackbody that provides thermal radiation from -173°C to 177°C and is described in detail in [5]. A schematic view of the VLTBB is given in Fig. 4. It features a liquid nitrogen-cooled and electrically heated outer thermostat for coarse temperature regulation. The fine regulation is done by three-zone heating of the cavity. Each zone features a dedicated PID temperature controller. The cavity is designed to maximize temperature uniformity along its walls. Seven platinum resistance thermometers (PRTs) are used for regulation. One is located at the thermostat and six are located along the cavity, two in each heating zone. One of the two is the sensor for the respective temperature controller, and the other allows independent monitoring of the temperature to correct the set point of the temperature controller. Another five

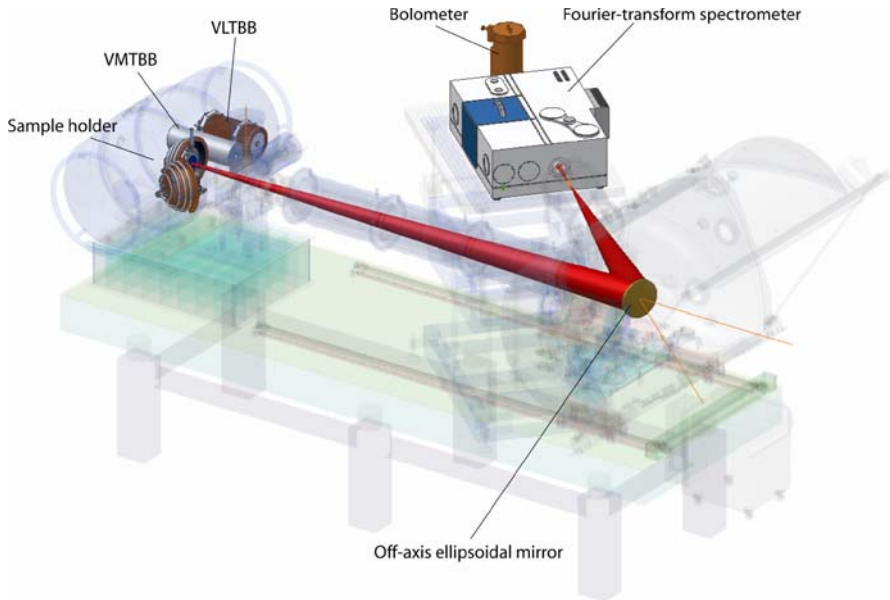


Fig. 3 Transparent view of the reduced-background facility to illustrate the position of the blackbodies and the sample holder, as well as the beam path, for spectrally resolved measurements. Radiation from either of the two blackbodies or the sample holder is imaged via the off-axis ellipsoidal mirror into the FTIR

sensors located along the cavity at different positions allow independent monitoring of the blackbody via a Hart Super-Thermometer Model 1590. The wires for all sensors feature an additional electrically isolated mounting point on the cavity near each sensor. The mounting point is approximately at the same temperature as the sensor. Thereby, the heat flow from and to the sensors via the wires is minimized. The PRTs were calibrated with a measuring current of 0.35 mA in the temperature range from $-71\text{ }^{\circ}\text{C}$ to $180\text{ }^{\circ}\text{C}$, and with a measuring current of 0.5 mA at temperatures of $0.01\text{ }^{\circ}\text{C}$ and $-196\text{ }^{\circ}\text{C}$ (77 K). For these measuring currents, the self-heating is included in the calibrations. For example, for a measurement at $0.01\text{ }^{\circ}\text{C}$ with a measuring current of 0.5 mA, the self-heating is 4.5 mK. At a temperature of 77 K, the self-heating with 0.5 mA is unknown because the change of the resistance value was negligible compared to the noise of the measurement and the resulting uncertainty of calibration. The temperature measurements with the PRT sensors at the VLTBB were made with a measuring current of 1 mA. The difference in self-heating of the PRT sensors as a result of the higher measuring current was not corrected in the measurements reported here.

2.2.2 Vacuum Variable Medium-Temperature Blackbody (VMTBB)

The VMTBB is a reference blackbody that will provide thermal radiation from $150\text{ }^{\circ}\text{C}$ to $430\text{ }^{\circ}\text{C}$ and it is currently under construction. It is of similar design as the VLTBB [5], with coarse temperature regulation via an electrically heated outer thermostat

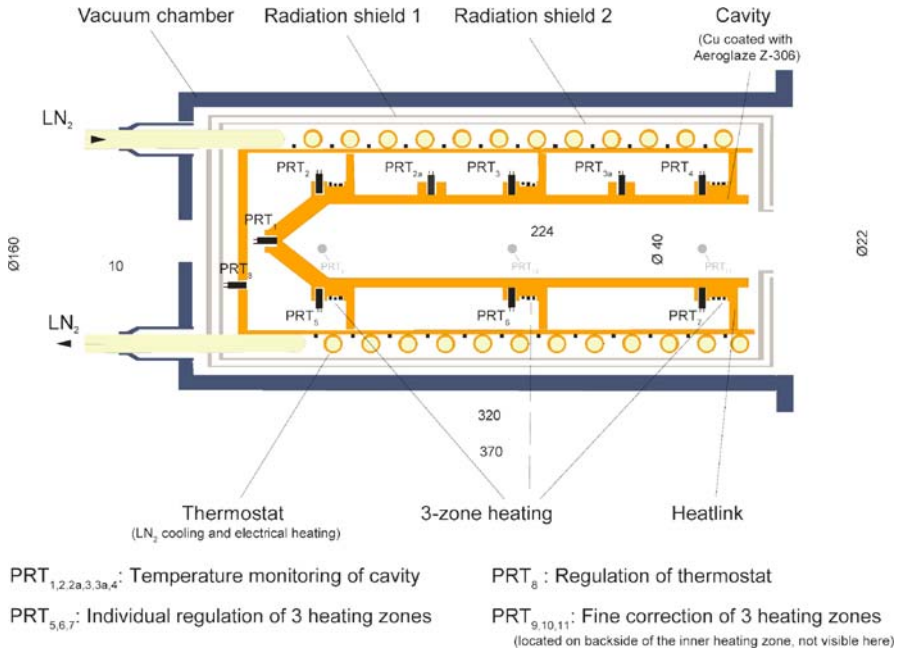


Fig. 4 Cutaway view through the VLTBB illustrating the construction with an outer thermostat and three inner heating zones. Also, the positions of all PRTs are indicated

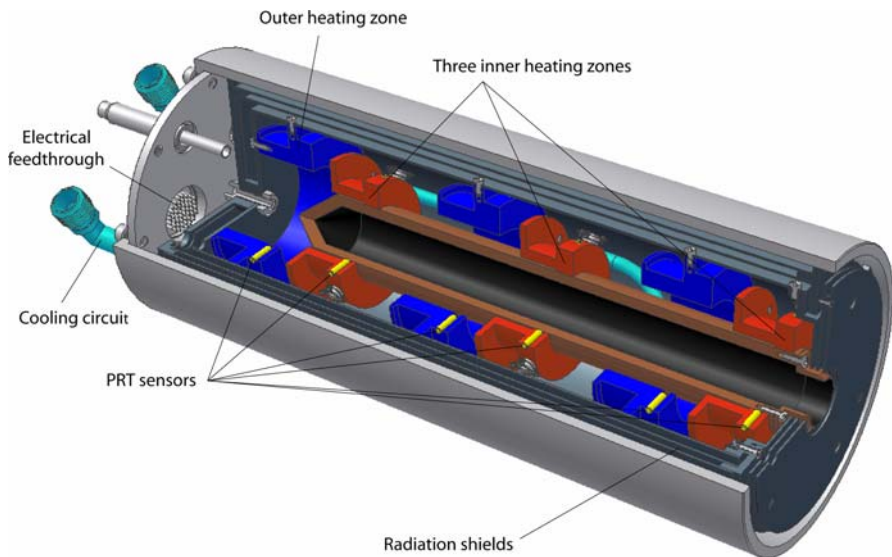


Fig. 5 The construction of the VMTBB. Several parts are highlighted. The three inner heating zones (red) have direct contact with the cavity. All possible PRT (yellow) positions are shown; however, not all sensor positions in the outer heating zone (blue) will be used. The three-fold radiation shield and the cooling circuit are also marked

Table 1 Specifications of the three blackbodies operated at the reduced background calibration facility

	VLBB	VMTBB ^a	Indium fixed point
Temperature (°C)	−173 to 177	150 to 430	156.5985 ^b
Emissivity	0.9997	0.9996	0.9999
Cavity material	Copper	Copper	Copper
Coating of wall	Aeroglaze Z306	Under Test	Pyromark 2500
Wall emissivity/diffusivity	0.95/0.82	0.92/0.8	0.96/0.8
Diameter of cavity (mm)	40	26	32
Diameter of cavity aperture (mm)	20	20	20
Length of cavity (mm)	250	240	153
Angle of bottom cone (°)	75	75	75
Temperature uniformity (mK)	<60	<100	
Temperature stability	<10 mK	<100 mK	80 mK · h ^{−1c}

^aAll values reported for the VMTBB are design parameters

^bDesign parameter

^cSlope of plateau of solidification, deviation from slope is much smaller

and fine regulation via three-zone heating of the cavity. It also features seven PRTs dedicated to regulation and three additional PRT sensors for independent monitoring of the cavity temperature. The blackbody has an additional cooling circuit that enables faster transitions toward lower temperatures. The construction of the blackbody is depicted in Fig. 5.

2.2.3 Indium Fixed-Point Radiator

The indium fixed-point radiator is of similar design as the gallium fixed point described in [4] with a copper cavity inside an indium-filled PTFE cell. The purity of the indium is at least 0.9999999.

An overview of the relevant specifications of the three blackbodies operated with the RBCF is given in Table 1.

2.2.4 Vacuum Sample Holder for Emissivity Measurements

A dedicated sample holder for emissivity measurements under vacuum was constructed. Samples are mounted on a plate of Inconel 600 which is heated from the back side by a bifilarly wound resistive heating wire. A typical sample is round with a diameter in the range from 40 mm to 100 mm and a thickness from 2 mm to 10 mm. Preferably, the samples should feature a radial hole of 1.8 mm diameter extending approximately 30 mm from the circumference of the sample to the center. Here, a temperature sensor can be placed to allow a more precise calculation of the heat flux through the sample and, in turn, a more precise determination of the surface temperature (see footnote in Sect. 1.3). Sample temperatures for emissivity measurements can be controlled in the range from 0 °C to 430 °C. The heated sample is located inside a spherical enclosure of 250 mm diameter made of copper that can be temperature controlled from about liquid nitrogen to room temperature and as such provides a known thermal environment. The

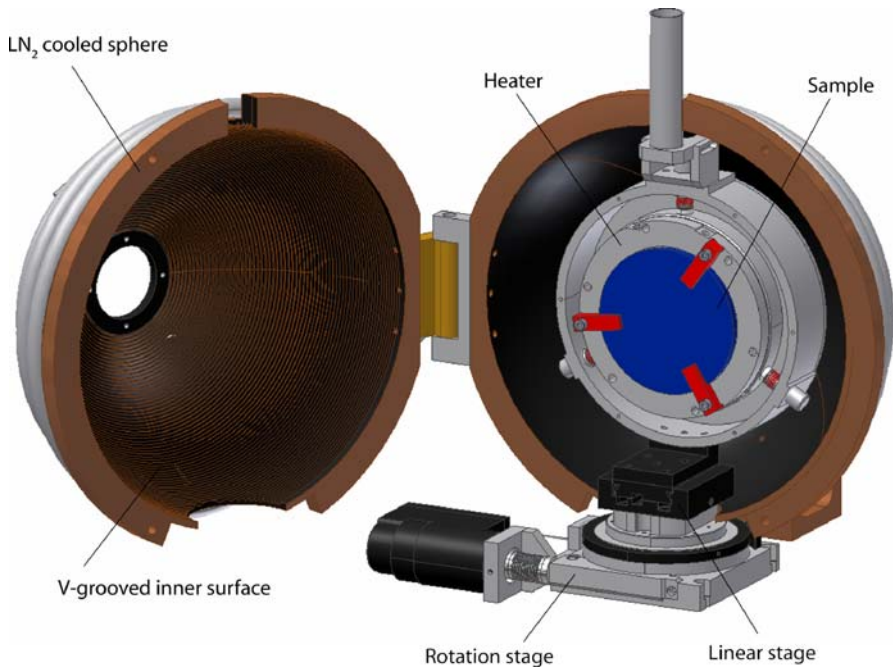


Fig. 6 Construction of the vacuum sample holder. Exchange of samples is facilitated by a door-like opening mechanism

inner surface of the sphere is covered by circular grooves (60°) and coated with Nextel 811-21 to provide an emissivity greater than 0.98. The sample can be rotated within the sample holder by a DC-motor-driven rotation stage without geometrical restrictions. However, depending on the results of size-of-source measurements with the vacuum FTIR, the useful range for emissivity measurements will probably be in the range of $\pm 75^\circ$. A small linear stage allows positioning of the sample surface in the axis of rotation for samples of different thickness. The construction of the sample holder is shown in Fig. 6.

2.2.5 Vacuum Infrared Standard Radiation Thermometer (VIRST)

VIRST has been designed for temperature measurements from -150°C to 170°C under vacuum in the spectral band from $8\ \mu\text{m}$ to $14\ \mu\text{m}$. The radiation thermometer is a purpose-built instrument to be operated with the RBCF as a transfer instrument for the comparison of temperature radiators with the RBCF reference blackbodies. Furthermore, VIRST is a stand-alone system with an air-tight housing that allows operation inside a vacuum chamber, attached to a vacuum chamber, or in air. This allows the VIRST to be used to compare the water- and ammonia-heat-pipe blackbodies of the PTB low-temperature calibration facility in air with the VLTBB under vacuum. Results of the comparison are given in Sect. 3. Finally, once sufficient

long-term stability has been proven for the instrument, VIRST will be used to carry and compare the temperature scale under vacuum of PTB to remote-sensing calibration facilities outside PTB. Details of VIRST are given in [2,6,7].

2.2.6 Vacuum Fourier-Transform Spectrometer (FTIR)

The vacuum Fourier-transform infrared spectrometer (FTIR) employed at the RBCF is a Bruker Vertex 80V. In our experiment, it covers the wavelength range from $1\ \mu\text{m}$ to $1,000\ \mu\text{m}$. Several detectors are employed, an InSb detector for the range from $1\ \mu\text{m}$ to $5\ \mu\text{m}$ and a MCT-detector from $2.5\ \mu\text{m}$ to $14\ \mu\text{m}$, both of which are liquid nitrogen-cooled standard detectors. Also, a pyroelectric DLATGS detector that is less sensitive, but easy to operate, will be used for the MIR/FIR range. The spectrometer will also feature a liquid helium-cooled Si-composite bolometer for the FIR range. The Si-composite bolometer is modified with respect to the standard Bruker bolometer. It has a wedged diamond window to cover a wavelength range from $10\ \mu\text{m}$ to $1,000\ \mu\text{m}$ and above. Also, three long-pass filters are employed with cut-on wave numbers (wavelengths) of $1000\ \text{cm}^{-1}$ ($10\ \mu\text{m}$), $370\ \text{cm}^{-1}$ ($27\ \mu\text{m}$), and $100\ \text{cm}^{-1}$ ($100\ \mu\text{m}$). To avoid saturation when working at $10\ \mu\text{m}$, the thermal conductivity of the lead wires of the bolometer element is increased by a factor of two. External radiation can be imaged into the spectrometer through an entrance port which features, in our case, a 90° off-axis parabolic mirror with an effective focal length of $250\ \text{mm}$.

2.2.7 Beam Path and Optical Elements

All critical elements in the optical path, like the baffles, aperture stop, and field stop, are liquid nitrogen cooled. If necessary, the detector chamber can also be equipped with a cold shield. The radiation from the blackbodies or the sample holder is imaged to the object point of the “entrance” off-axis parabolic mirror of the spectrometer by an off-axis ellipsoidal mirror. The gold-coated ellipsoidal mirror has a diameter of $160\ \text{mm}$ and features a bending angle of 40° and effective focal lengths of $2,758\ \text{mm}$ and $1,400\ \text{mm}$. If necessary, it is possible to place a liquid nitrogen-cooled aperture at the intermediate focal point between the two mirrors. At this location, two different vacuum regimes have to be separated, the spectrometer regime which is operated around $10^2\ \text{Pa}$ and the RBCF which is operated at $10^{-2}\ \text{Pa}$. Due to the high pressure difference and the diameter of the beam waist of approximately $10\ \text{mm}$ at this position, differential pumping was not applicable and a window has to be used. Here, this is realized by two windows, a wedged diamond window and a wedged ZnSe window, mounted on a vacuum-tight sliding mechanism. Both materials feature the same index of refraction of 2.41 at the wavelength changeover of $10\ \mu\text{m}$. They also have the same wedge angle of 0.5° , which ensures a similar beam deviation. Both windows are thermally stabilized by liquid cooling. If necessary, they could also be cooled to liquid nitrogen temperature.

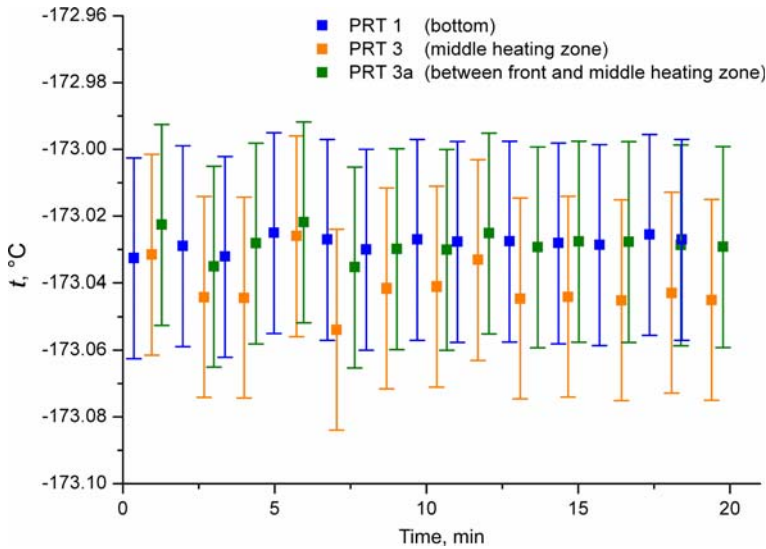


Fig. 7 Stability of the VLTBB at $-173.03\text{ }^{\circ}\text{C}$. The given uncertainty ($k = 2$) is the uncertainty of the calibration of the PRTs used for temperature monitoring of the VLTBB. For 20 min, three sensors located along the cavity were monitored with a Hart Super-Thermometer Model 1590. The stability and temperature uniformity of the VLTBB are within the calibration uncertainty of the sensors

3 Measurement Schemes and First Results

The following measurement schemes are possible at the reduced background facility:

- Radiators can be compared with dedicated reference blackbodies.
 - Via VIRST, in terms of radiation temperature in the spectral band (8–14) μm .
 - Via the vacuum FTIR, spectrally resolved in terms of spectral radiance.
- Radiation detectors can be characterized with the two blackbodies as primary sources of thermal radiation in the range from $-173\text{ }^{\circ}\text{C}$ to $430\text{ }^{\circ}\text{C}$.
- The directional spectral emissivity of samples can be determined in the temperature range from $0\text{ }^{\circ}\text{C}$ to $430\text{ }^{\circ}\text{C}$ and wavelength range from $1\text{ }\mu\text{m}$ to $1,000\text{ }\mu\text{m}$ by comparison to two reference blackbodies.

In the following, the first experimental results and a theoretical data analysis scheme are presented.

3.1 Stability of the VLTBB

The stability of the blackbody was determined by monitoring three of its additional PRT sensors over different time intervals. One of the measurements is shown in Fig. 7. Within the calibration uncertainty of the sensors of 30 mK ($k = 2$) and the long-term stability of the sensors of $50\text{ mK}\cdot\text{year}^{-1}$, one can state that the blackbody is stable and isothermal.

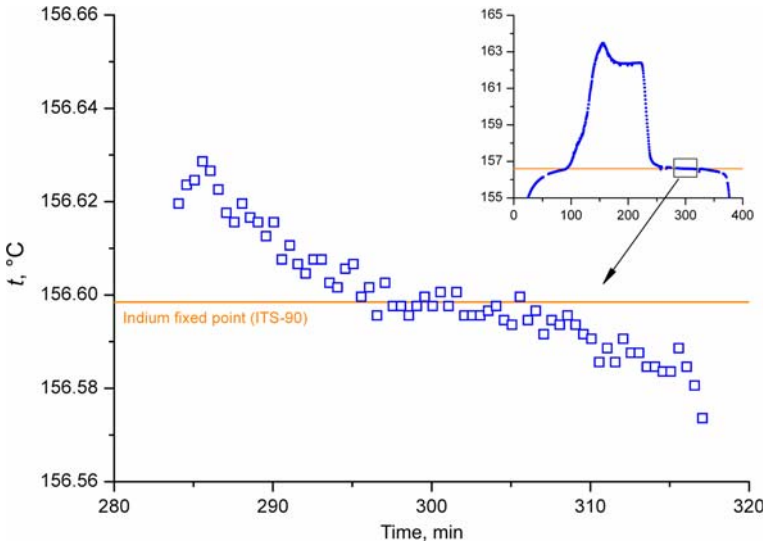


Fig. 8 Solidification of the indium fixed-point radiator observed with VIRST. In the inset, the whole melting and solidification cycle is depicted. In the main graph, a part of the solidification plateau is shown from which a slope of $80\text{mK}\cdot\text{h}^{-1}$ can be estimated. The measured data are corrected for the observation via a gold mirror which still has to be calibrated. Here, a reflectivity of the gold mirror of 0.97 is assumed

3.2 Solidification Plateau of the Indium Fixed-Point Blackbody

The melting and solidification plateaux were measured with the VIRST instrument via a gold mirror. A typical plateau of solidification lasts at least 1 h with a remaining slope of about $80\text{mK}\cdot\text{h}^{-1}$. In Fig. 8, a melting and solidification cycle is depicted. The slope of the melting “plateau” and the shoulder at its end indicates a possible non-uniformity of the temperature along the cavity during the melting process. The relative low thermal conductivity of PTFE and the large opening of the radiating cavity could be possible reasons for this behavior.

3.3 Reduction of Background Radiation by the Cooled Beamline

To illustrate the effect of the cooled beamline, measurements of the radiation temperature of the VLTBB were performed with VIRST. The measurement area of VIRST was scanned from -30mm to $+30\text{mm}$ with respect to the center of the VLTBB. The measurements were performed with and without liquid nitrogen (LN_2) cooling of the beam line. The results are shown in Fig. 9. The plateau indicates the range when the measurement area of VIRST, with a diameter of 10mm , is “inside” the 20mm cavity opening of the VLTBB. When VIRST starts ‘seeing’ the blackbody aperture, the measured temperature drops. The reduced temperature in the vicinity of the aperture in the case of the cooled beamline is clearly visible. The center height of the plateau deviates negligibly for both measurements because of the relatively small size-of-source effect of VIRST.

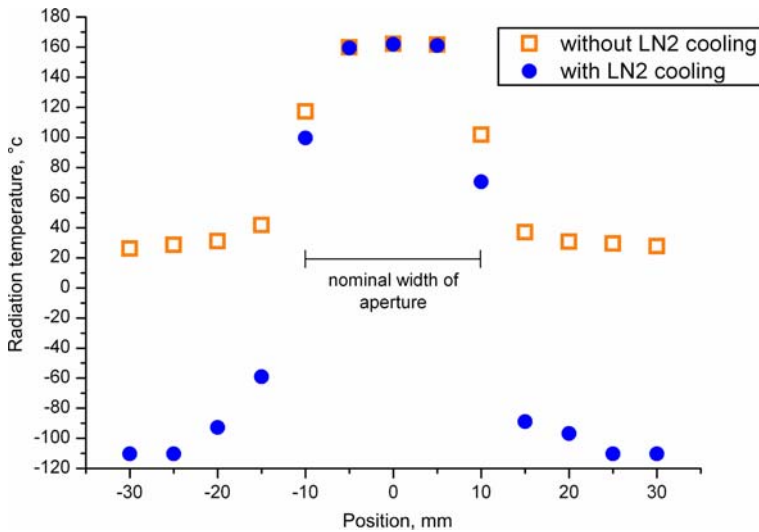


Fig. 9 Radiation temperature of the VLTBB measured by VIRST. The measurement area is scanned over an interval from -30 mm to $+30\text{ mm}$ with respect to the center of the VLTBB. The distribution of the radiation temperature is shown for the cases with and without liquid nitrogen cooling of the beamline. Clearly visible is the reduced temperature in the vicinity of the cavity. For these measurements, VIRST was operated at 23°C , which limits the measurement range to the interval from -120°C to 170°C

3.4 Flux into the FTIR

In Fig. 10, the flux of the two blackbodies at 300 K and 600 K , detected by the FTIR within a bandpass of 1 cm^{-1} , is simulated. Three calculations with different spatial resolutions of 10 mm , 1 mm , and 0.1 mm at the sample surface are shown. For comparison, the noise equivalent power (NEP) of the spectrometer is also shown. It is calculated from the NEP of the individual detectors and an estimation of the transmittance of the spectrometer. Apparently, good dynamic ranges with three orders of magnitude can be reached for temperatures of 600 K and spatial resolutions of 1 mm for the range from $3\text{ }\mu\text{m}$ to $40\text{ }\mu\text{m}$. For a temperature of 300 K , this is only achievable with reduced spatial resolution.

3.5 Elimination of Background Radiation by Measurement with Respect to Two Blackbodies

Generally, a measured signal for the directional spectral emissivity $\tilde{L}_{\text{Sample}}$ is of the form,

$$\begin{aligned} \tilde{L}_{\text{Sample}}(T_{\text{Sample}}) = & s \left(\varepsilon_{\text{Sample}} L_{\text{Planck}}(T_{\text{Sample}}) \right. \\ & + \rho_{\text{Sample}} \varepsilon_{\text{Environment}} L_{\text{Planck}}(T_{\text{Environment}}) \\ & \left. - \varepsilon_{\text{Detector}} L_{\text{Planck}}(T_{\text{Detector}}) + L_{\text{Background}} \right) \end{aligned}$$

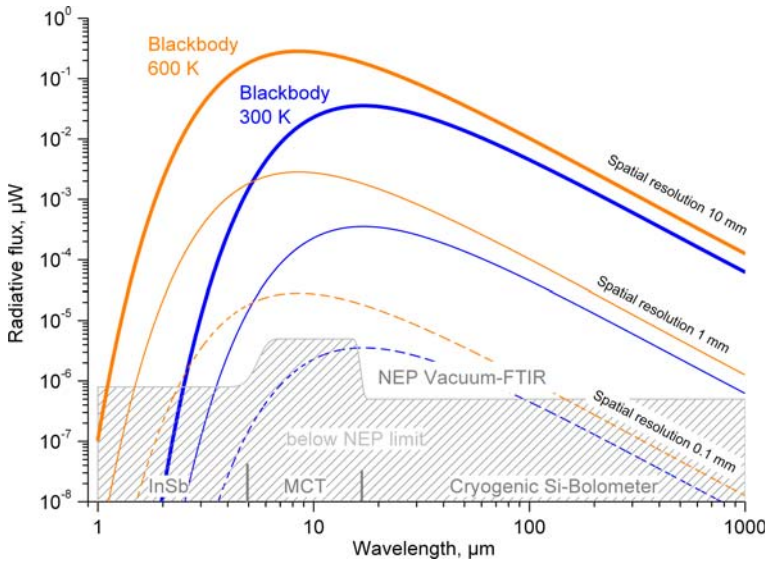


Fig. 10 Calculated flux into the vacuum FTIR originating from blackbodies at 300 K and 600 K. Depicted are the cases with spatial resolutions of 10 mm, 1 mm, and 0.1 mm at the blackbody opening or sample surface, respectively. The calculation assumes a bandwidth of 1 cm^{-1} and a recording time of 1 s. For comparison, the estimated noise-equivalent power (NEP) of the spectrometer is also shown

Here s denotes the spectral responsivity of the spectrometer, $L_{\text{Planck}}(T)$ is the spectral blackbody radiance at the respective temperature, ϵ_{Sample} is the desired directional spectral emissivity of the sample, $\epsilon_{\text{Environment}}$ and $\epsilon_{\text{Detector}}$ are the directional spectral emissivities of the environment and detector, and $L_{\text{Background}}$ is the spectral thermal background radiance. By providing an isothermal environment of homogenous emissivity, the directional-hemispherical spectral reflectivity ρ_{Sample} of an opaque sample can be substituted by the directional spectral emissivity, $\rho_{\text{Sample}} = 1 - \epsilon_{\text{Sample}}$, which yields

$$\begin{aligned} \tilde{L}_{\text{Sample}}(T_{\text{Sample}}) = & s (\epsilon_{\text{Sample}}L_{\text{Planck}}(T_{\text{Sample}}) \\ & + (1 - \epsilon_{\text{Sample}})\epsilon_{\text{Environment}}L_{\text{Planck}}(T_{\text{Environment}}) \\ & - \epsilon_{\text{Detector}}L_{\text{Planck}}(T_{\text{Detector}}) + L_{\text{Background}}) \end{aligned}$$

In the case of the reference blackbodies, one can assume $\epsilon_{\text{Sample}} \approx 1$ and the signal simplifies to

$$\tilde{L}_{\text{BB}}(T_{\text{BB}}) = s (L_{\text{Planck}}(T_{\text{BB}}) - \epsilon_{\text{Detector}}L_{\text{Planck}}(T_{\text{Detector}}) + L_{\text{Background}})$$

By forming the ratio of the sample measurement to one for the reference blackbody, $Q = \tilde{L}_{\text{Sample}}(T_{\text{Sample}})/\tilde{L}_{\text{BB}}(T_{\text{BB}})$, the spectral responsivity s cancels out. With known sample, detector, environment, and blackbody temperatures, as well as known spectral emissivities of the detector $\epsilon_{\text{Detector}}$ and of the environment $\epsilon_{\text{Environment}}$, and neglecting

the thermal background $L_{\text{Background}}$, the directional spectral emissivity of the sample $\varepsilon_{\text{Sample}}$ can be calculated from the measured quotient Q :

$$\varepsilon_{\text{Sample}} = \frac{Q (L_{\text{Planck}}(T_{\text{BB}}) - \varepsilon_{\text{Detector}} L_{\text{Planck}}(T_{\text{Detector}})) + \varepsilon_{\text{Detector}} L_{\text{Planck}}(T_{\text{Detector}}) - \varepsilon_{\text{Environment}} L_{\text{Planck}}(T_{\text{Environment}})}{L_{\text{Planck}}(T_{\text{Sample}}) - \varepsilon_{\text{Environment}} L_{\text{Planck}}(T_{\text{Environment}})}$$

The thermal background cannot be neglected for emissivity measurements at low temperatures. However, the two variable-temperature reference blackbodies of the RBCF enable measurements of the emissivity of the sample with respect to two reference temperatures. One blackbody is operated close to the sample temperature T_{Sample} and the other one at a temperature T_{BB1} different from the sample temperature. By using the quotient of the two differences:

$$Q = \frac{\tilde{L}_{\text{Sample}}(T_{\text{Sample}}) - \tilde{L}_{\text{BB1}}(T_{\text{BB1}})}{\tilde{L}_{\text{BB2}}(T_{\text{Sample}}) - \tilde{L}_{\text{BB1}}(T_{\text{BB1}})}$$

the spectral responsivity s as well as the thermal background $L_{\text{Background}}$ of each radiance measurement can be eliminated, and compensation for disturbances by background radiation, resulting, for example, from inside the vacuum FTIR, is possible. Due to the phase lag of all the individual radiation components of a single measurement, the calculation of the directional spectral emissivity $\varepsilon_{\text{Sample}}$ has to be done with complex-valued radiances when using the FTIR [8,9]. The presented analysis assumes a linear behavior of the detectors. This is a reasonable assumption for the DLaTGS detector and the bolometer. However, the MCT and InSb detectors have to be corrected for their nonlinear behavior before using them in a linear analysis. Calculation of the spectral responsivities of the spectrometer for different temperature pairs of the two blackbodies will serve as a consistency check for the assumption of linearity.

4 Traceability

The traceability of calibrations performed at the RBCF is ensured via the PRTs of both blackbody radiators. These PRTs are calibrated against the fixed points of the ITS-90. For the VLTBB, an effective emissivity was calculated from a Monte-Carlo simulation of radiation in the cavity [5] and the temperature distribution of the cavity. By taking into account this effective emissivity and the thermal conductivity of the walls of the cavity, the uncertainty of the radiation temperature of the VLTBB can be given. The expanded uncertainty is shown for the range of operation from -130°C to 177°C as the gray area in Fig. 11.

As a check of consistency, the radiation temperature of the blackbodies can also be determined by VIRST, which is calibrated via the PTB heat-pipe blackbodies. We have performed this check with the VLTBB. The differences of the VIRST measurements and the radiation temperatures calculated from the PRT sensors of the blackbody are also depicted in Fig. 11. Within the temperature range from -20°C to 170°C and at -120°C , consistency within the combined uncertainty of the blackbody radiation

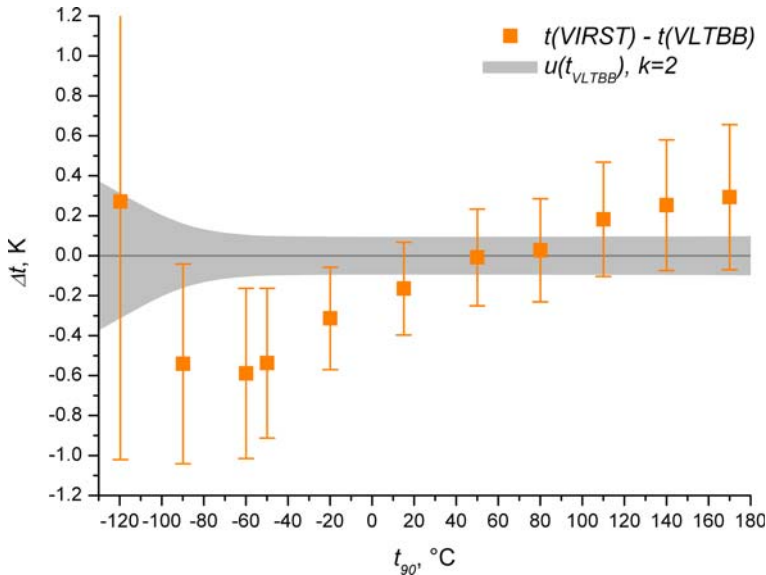


Fig. 11 The difference of temperatures of the VLTBB measured with its PRTs $t(\text{VLTBB})$ and the radiation temperature measured with VIRST $t(\text{VIRST})$. The given uncertainty ($k = 2$) is the combined uncertainty of the VIRST calibration at the low-temperature radiation facility, the uncertainty of the radiation temperature of the VLTBB, and that of the measurement process. VIRST was calibrated for the temperature range from -20°C to 170°C . For the measurements at the lower VLTBB temperatures from -50°C to -120°C , its reference function [6] was extrapolated. Gray area illustrates the uncertainty component of the radiation temperature of the VLTBB determined by its PRTs

temperature and the VIRST calibration is achieved. The slight deviations at -50°C , -60°C , and -90°C are probably due to the fact that the reference function of VIRST was

determined in the temperature range from -20°C to 170°C [6] and had to be extrapolated for the low-temperature comparisons. For the calculation of the interpolated reference function from -20°C to 170°C , integrated transmissions of the ZnSe windows and the Ge aspheric lens of VIRST have been used. For extrapolation of the reference function to temperatures below -20°C , knowledge of the correct spectral transmission of both elements would have been mandatory since the radiation contribution from them becomes significant. The uncertainty of this extrapolation is not yet included in the combined uncertainty shown in Fig. 11, and its inclusion might yield consistency within the expanded uncertainty.

5 Conclusion

PTB has started to operate a reduced-background calibration facility. At the time of writing, we are able to provide a scale of radiation temperature under vacuum from -173°C to 177°C . The stability of the operating dedicated vacuum reference blackbody (VLTBB) is within $\pm 30\text{mK}$. The expanded uncertainty for its radiation tempe-

perature in the range from -60°C to 177°C is below 100 mK. For the temperature range from -20°C to 170°C , the radiation temperature under vacuum is consistent with the established low-temperature radiation scale of PTB based on heat-pipe blackbodies [2]. With further improvement of the calibration of VIRST [6], we intend to perform a high-accuracy comparison of both scales at the level of uncertainty currently achieved for the radiation temperature of the VLTBB.

References

1. G. Ohring, B. Wielicki, R. Spencer, B. Emery, R. Datla, *Bull. Am. Meteorol. Soc.* **86**, 1303 (2005)
2. J. Hollandt, R. Friedrich, B. Gutschwager, D.R. Taubert, J. Hartmann, *High Temp. High Press.* **35/36**, 379 (2003/2006)
3. J. Lohrengel, R. Todtenhaupt, M. Ragab, *Wärme- und Stoffübertragung* **28**, 6 (1993)
4. V.S. Ivanov, B.E. Lisiansky, S.P. Morozova, V.I. Sapritsky, U.A. Melenevsky, L.Y. Xi, L. Pei, *Metrologia* **37**, 599 (2000)
5. S. Morozova, N.A. Parfentiev, B.E. Lisiansky, V.I. Sapritsky, N.L. Dovgilov, U.A. Melenevsky, B. Gutschwager, C. Monte, J. Hollandt, in *Proceedings of TEMPMEKO 2007*, *Int. J. Thermophys.* **29**, 341 (2008). doi:[10.1007/s10765-007-0355-z](https://doi.org/10.1007/s10765-007-0355-z)
6. B. Gutschwager, J. Hollandt, T. Jankowski, R. Gärtner, in *Proceedings of TEMPMEKO 2007*, *Int. J. Thermophys.* **29**, 330 (2008). doi:[10.1007/s10765-007-0349-x](https://doi.org/10.1007/s10765-007-0349-x)
7. J. Hollandt, B. Gutschwager, T. Jankowski, R. Gärtner, in *TEMPERATUR 2006*, ed. by J. Hollandt, S. Rudtsch (Berlin, 2006), pp. 71–79
8. H.E. Revercomb, H. Buijs, H.B. Howell, D.D. LaPorte, W.L. Smith, L.A. Sromovsky, *Appl. Optics* **27**, 3210 (1988)
9. L.A. Sromovsky, *Appl. Optics* **42**, 1779 (2003)